

# Behavior of a geogrid reinforced soil wall built with clayey silt

Sayão, A.S.F.J.

*PUC-Rio, Catholic University of Rio de Janeiro, Brazil*

Becker, L.B.

*UFRJ, Federal University of Rio de Janeiro, Brazil*

Nunes, A.L.L.S.

*COPPE-UFRJ, Federal University of Rio de Janeiro, Brazil*

Costa Filho, L.M.

*LPS Consultoria e Engenharia Ltda, Rio de Janeiro, Brazil*

Keywords: Geogrids, Reinforced Soil, Retaining Wall, Finite Element Method, Numerical Simulation.

**ABSTRACT:** This paper presents the construction details of a reinforced retaining wall 5m high, made as part of a 1700m long earth fill dyke for containing bauxite residues in Minas Gerais, Brazil. The reinforced wall was built with compacted clayey silt residual soil available locally. Geogrids with a vertical spacing of 0.40 to 0.60m were used as reinforcing elements. The wall was instrumented with surface marks and tell-tales, for monitoring construction displacements at the face and within the soil mass. A numerical simulation of the construction process was carried out with the Plaxis computer program, which is based on the finite element method. Pull out tests were conducted in a experimental fill and its results were used to validate the numerical models and parameters. Predictions of surface and inner displacements are shown to agree reasonably well with field measurements of the wall. Tensile loads in the geogrids were estimated from measured field strains. These were also close to the values predicted from the numerical simulations.

## 1 INTRODUCTION

Numerical analysis of reinforced soil structures may provide estimates of displacements, strains and stresses for a variety of load conditions. Bathurst et al. (2002), Pereira and Palmeira (2005), and Vicari and Silva (2005) present numerical analysis of reinforced soil during and after compaction.

Under usual service conditions of reinforced soil structures, relative displacement between soil and reinforcement is negligible. Rowe e Ho (1998) presented numerical evaluations of soil and reinforcement displacements, noting that differential strains only occurred for the upper reinforcement layer, under very low confining stress. This conclusion was valid for different values of reinforcement stiffness and soil strength.

Analytical models, capable of reproducing both load transfer and displacement mechanisms on the geogrid length, have been proposed (Sieira et al., 2009). This paper presents a comparison between numerical predictions and measured values from field monitoring of a reinforced soil wall.

## 2 REINFORCED SOIL WALL

At the ALCOA aluminum plant, in Minas Gerais State (Brazil), bauxite residue disposal areas (RDA) were built with containment earth fill dikes. RDA no. 7 was formed by a closed dyke about 13m high, creating a lake of 1700m perimeter and  $1.5 \times 10^6 \text{m}^3$  volume. Impermeable layers were placed at the lake bottom and at the dyke's inner slopes, for avoiding underground contamination by caustic fluid seepage.

Due to topographical restrictions, the available location for the construction of RDA no. 7 would imply excessively long earth fills. Therefore, a solution was developed with a reinforced soil wall at the upper 5m of the perimeter dikes. This solution significantly reduced the volume of earth fills and the environmental impact in the area. More details are reported by Becker (2006) and Costa Filho and Sieira (2008).

A typical cross-section of the wall is presented in Figure 1. Inclination of the face is 1H : 5V. A locally available clayey silt residual soil (PI=23%) was compacted in layers (Figure 2) to an average compaction degree of 98% of Standard Proctor.

Soil reinforcement was provided by PVA geogrids specially manufactured to resist the caustic liquor present in the bauxite tailings (Silva et al., 2008). Table 1 shows the nominal properties of the geogrids, from wide width tensile tests.

A detailed investigation on the field pullout resistance of these geogrids was carried out in an experimental fill with the same soil (Becker et al., 2008).

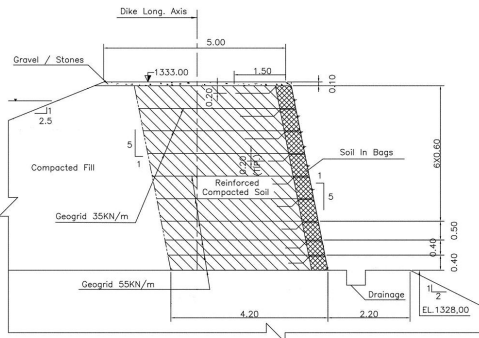


Figure 1. Typical cross section of the reinforced fill



Figure 2. Construction of the geogrid reinforced wall

Table 1. Geogrid nominal properties (Becker, 2006)

Geogrid Description	Tensile Strength (kN/m)	Elongation at failure (%)	Longitudinal Stiffness (kN/m)
Fortrac 35/20	35	5	700
Fortrac 55/25	55	5	1100

Construction procedure consisted of placing the geogrid within the compacted soil layers. Geogrid 55 was used at the six lower layers (0.4m spacing). Geogrid 35 (top three layers) had 0.6m spacing.

The reinforced wall had two sections instrumented. Vertical and horizontal displacements at the face were monitored with surface marks during and after construction.

In each instrumented section, horizontal displacements were monitored by tell-tales at three selected geogrid layers. These geogrids were placed at a height of 40, 190 e 370 cm. As shown in Figure 3,

six tell-tales were installed in the two lower grids, while the upper grid had eight tell-tales.

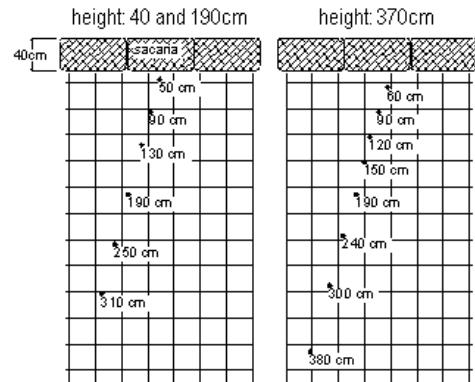


Figure 3. Position of tell-tales along the horizontal geogrids, in relation to the frontal face of the wall (Becker, 2006)

### 3 NUMERICAL ANALYSIS

The construction of the reinforced wall was simulated with the computational program Plaxis 2D v.8 (Brinkgreve e Vermeer, 1998), based on the finite element method. The geometry of the instrumented section is presented in Figure 4. The reinforced wall and the compacted clayey silt backfill are shown at the upper part of the earth dyke.

The stress-strain behavior of the compacted soil was simulated by the Hardening Soil model. This model uses a hyperbolic formulation and incorporates concepts of plasticity and dilatancy, as an improvement of the traditional model proposed by Duncan et al (1980). Soil parameters were derived from oedometer and triaxial compression test results (Becker, 2006) and are presented in Table 2.

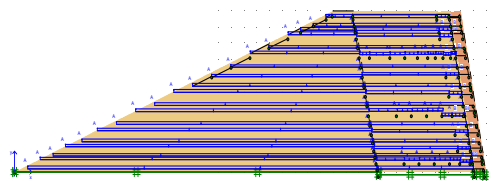


Figure 4. Geometry adopted for the numerical analysis

For simulating the reinforcement, Plaxis offers a special element. As input data, it requires only the longitudinal stiffness from wide-width tensile tests.

The numerical simulations tried to duplicate closely the construction sequence, with one loading stage representing each compacted soil layer and geogrid. At several stages, predicted displacements and field measurements were compared at specific points of the wall face and the geogrid.

Table 2. Parameters of compacted clayey silty soil

$\gamma$ (kN/m <sup>3</sup> )	$\phi$ (°)	$\psi$ (°)	c (kPa)	$E_{50}^{ref}$ (MPa)	$E_{oed}^{ref}$ (MPa)	$E_{ur}^{ref}$ (MPa)
18	34	2.7	10	9.5	9.5	28.0

$\gamma$  = unit weight of soil,  $\phi$  = friction angle,  $\psi$  = dilatancy angle, c = cohesion,  $E_{50}^{ref}$  = young's modulus,  $E_{oed}^{ref}$  = oedometer modulus,  $E_{ur}^{ref}$  = unload-reload modulus

## 4 ANALYSIS OF RESULTS

### 4.1 Face Displacements

Figure 5 confronts measured and predicted horizontal displacements at the wall face, at 450cm of wall height. A fairly good agreement may be noted. The ratio  $D_H/H$  (maximum horizontal face displacement over the wall height) was found to be about 1.1%.

The small movements observed during construction were mainly due to the high stiffness of the geogrids and to the low deformability of the clayey silty fill. In the 5 years after construction, overall behavior along the wall has been very good, with no signs of distress (Costa Filho and Sieira, 2008).

The zero horizontal displacement shown at the toe of the wall was caused by fixities applied to the base of the wall in the numerical simulation and are not expected in real walls. However, this condition was assumed due to the high inertia of the embedded reinforced concrete ditch that lies in front of the wall toe.

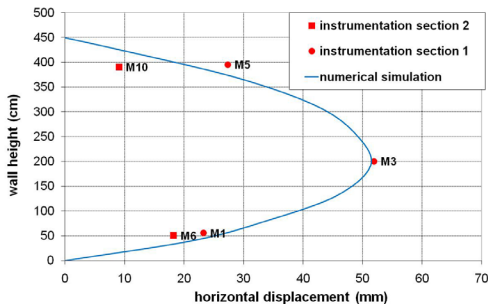


Figure 5. Comparison of predicted and measured horizontal face displacements at different wall elevations

### 4.2 Inner displacements of the geogrid

Figures 6 to 8 present inner displacements given by tell-tales along the geogrids at 450cm of wall height.

At the upper geogrid, at elev. 370cm (Figure 6), all tell-tales worked properly. At elevations 190 and 40cm (Figures 7 and 8, respectively), some readings were disregarded due to mal-functioning of tell-tales far from the wall face. Nevertheless, a fairly reasonable agreement between numerical predictions and

measured values may be noted for the central geogrid. At the upper and lower geogrids (elev. 370 and 40cm), agreement between measured and predicted values was not as good.

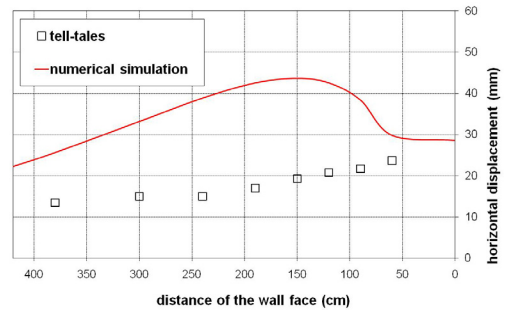


Figure 6. Predicted and measured horizontal displacements along the upper geogrid (elev. 370cm)

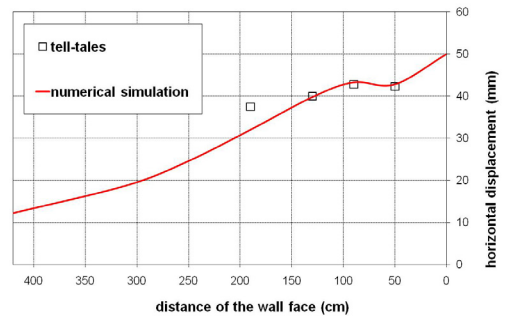


Figure 7. Predicted and measured horizontal displacements along the central geogrid (elev. 190cm)

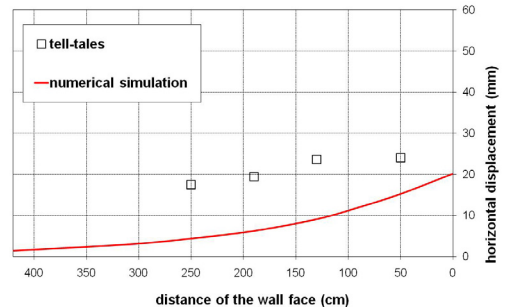


Figure 8. Predicted and measured horizontal displacements along the lower geogrid (elev. 40cm)

### 4.3 Tensional loads

Based on the strains computed from adjacent tell-tales, tensile loads along the geogrid may be estimated. Table 3 shows a comparison between the maximum tensional loads measured and predicted by numerical simulation in the geogrids (Becker, 2006).

Table 3. Maximum tensional loads in the geogrids

Geogrid type	Elevation in the wall (cm)	Tensile strength (kN/m)	Measured maximum load (kN/m)	Predicted maximum load (kN/m)
F 35	370	35	5.1	7.9
F 55	190	55	8.5	14.2
F 55	40	55	8.5	13.9

From Table 3, it is observed that maximum mobilized tensile loads were about 15% (measured) or 25% (predicted) of the wide width tensile strength. These values do not account neither for creep effects, chemical or biological degradation or installation damage nor for desired deformations.

It should be noted that these load estimates, made from measured displacements, are average values over the region considered. No localized values can be obtained and therefore the load distribution along the reinforcement is somewhat lost. Furthermore, in rigid geogrids, tell-tales measurements exhibit a lower accuracy, which is carried on to the load estimates. This is mostly important in the early construction stages, where mobilized displacements are small. Therefore it would be reasonable to expect that measured tensile loads were lower than the predicted ones.

## 5 CONCLUSIONS

This paper presents a comparative analysis between predicted and measured construction behaviors of a reinforced soil wall. Numerical simulations were carried out with the program Plaxis. The wall was built with compacted clayey silt reinforced with geogrids. Field instrumentation was done with surface marks on the wall face and tell-tales installed along the geogrids.

It is shown that the displacements during construction compared fairly well. Numerical predictions of geogrid loads were not much higher than tensile loads inferred from measured displacements in the field.

The maximum horizontal face displacement was found to be about 1.1% of the wall height, confirming the safe performance of the geogrid reinforced wall.

## ACKNOWLEDGEMENTS

The authors are indebted to Alcoa (Brazil) and Huesker (Brazil) for all the support with the field monitoring and testing program at the residue deposit. Financial support from CNPq (Brazilian Research Council) is also gratefully acknowledged.

## REFERENCES

- Bathurst R.J., Walters D.L., Hatami K., Saunders D., Vlachopoulos N., Burgess G.P., Allen T. (2002). Performance testing and numerical modelling of reinforced soil retaining walls. 7<sup>th</sup> International Conference on Geosynthetics. Nice, pp.217-220.
- Becker, L.B. (2006). Behavior of geogrids in a reinforced wall and in pullout tests (in Portuguese). Doctoral thesis. PUC-Rio, Catholic University of Rio de Janeiro, Brazil, 322p.
- Becker, L.B., Sayão A.S.F.J., Nunes A.L.L.S., Costa Filho L.M. (2008). Characterization of soil-geogrid interface strength in reinforced mass (in Portuguese). 4<sup>th</sup> Luso-Brazilian Conference on Geotechnics. Coimbra, Portugal.
- Brinkgreve R.J.B., Vermeer P.A. (1998). Finite element code for soil and rock analyses – Plaxis 2D user’s manual. Balkema. Rotterdam.
- Costa Filho L.M., Seira A.C.C.F. (2008). Recent Applications of Geosynthetics in Mining and Industrial Waste Disposal. 1<sup>st</sup> PanAmerican Geosynthetics Conf., Cancun, Mexico, v.1, pp.29-44.
- Duncan J.M., Byrne P., Wong K., Mabry P. (1980). Strength, stress-strain and bulk modulus parameters for finite element analysis of stresses and movements in soil masses. Geotechnical Engineering Research Report UCB/GT/80-01. University of California. Berkeley, USA.
- Pereira U.A., Palmeira E.M. (2005). Comparisons of methods for predicting displacement and loads in geosynthetic reinforced walls (in Portuguese). 5<sup>th</sup> Brazilian Symposium on Computational Applications in Geotechnics. Belo Horizonte, Brazil, pp. 315-319.
- Rowe R.K., Ho S.K. (1998). Horizontal deformation in reinforced soil walls. Canadian Geotechnical Journal. v. 35, pp.312-327.
- Seira A.C.C.F., Gerscovich D.M.S., Sayão A.S.F.J. (2009). Displacement and load transfer mechanisms of geogrids under pullout condition. Geotextiles & Geomembranes, Elsevier, v.27, pp.241-253.
- Silva A.E., Schmidt C., Costa Filho L.M., Becker L. B. (2008). Geogrid reinforced dyke in a chemically aggressive residue disposal area (in Portuguese). 14<sup>th</sup> Brazilian Conference on Soil Mechanics and Geotechnical Engineering, Búzios, Brazil, v.2.
- Vicari M., Silva J.D. (2005). Lessons learned from the numerical modelling of a retaining wall with non-uniform reinforcements. 5<sup>th</sup> Brazilian Symposium on Computational Applications in Geotechnics. Belo Horizonte, Brazil, pp.333-338.